Implementation of Grid-interactive Current Controlled Voltage Source Inverter for Power Conditioning Systems

Sung-Hun Ko† , Young-Chan Shin* and Seong-Ryong Lee**

Abstract - Increasing of the nonlinear type power electronics equipment, power conditioning systems (PCS) have been researched and developed for many years in order to compensate for harmonic disturbances and reactive power. PCS's not only improve harmonic current and power factor in the ac grid line but also achieves energy saving used by the renewable energy source (RES).
In this paper, the implementation of a current controlled voltage source inverter (CCVSI) using RES for PCS is presented. The basic principle and control algorithm is theoretically analyzed and the design methodology of the system is discussed. The proposed system could achieve power quality control (PQC) to reduce harmonic current and improve power factor, and demand side management (DSM) to supply active power simultaneously, which are both operated by the polarized ramp time (PRT) current control algorithm and the grid-interactive current control algorithm. A 1KVA test model of the CCVSI has been built using IGBT controlled by a digital signal processor (DSP). To verify the proposed system, a comprehensive evaluation with theoretical analysis, simulation and experimental results is presented.

Keywords: CCVSI, Demand side management, PCS, Power quality control

1. Introduction

Power conditioning systems (PCS) using renewable energy sources (RES) have been known as one of the most cost-effective, reliable and durable power systems to provide energy saving and high power quality. These grid-interactive PCSs can be classified as the series processing and parallel processing system according to the connection types of their output to other ac sources and loads. Typical examples of other ac sources are grid power and other RES sources. Recently, the parallel processing system using PCS has become more popular. As it is inherently efficient, compact and economical, it offers numerous functions requiring a minimum number of power conversions [1-5].

The grid-interactive PCS mainly controls the power flow and quality by the bi-directional Voltage Source Inverter (VSI) since it has to control the power conversion between the dc voltage source and the grid for RES applications. VSIs are intrinsically efficient, compact and economical devices to control power flow and provide quality supply [6-7]. The VSIs have two broad categories of inverter control techniques, which are voltage control and current control [8]. The current controlled voltage source inverter (CCVSI) is widely used in grid-interactive PCSs because the CCVSI can achieve unity power factor and can satisfy the total harmonic distortion (THD) of voltage and current in the entire load condition without an additional controller. And the CCVSI is faster in response compared with the voltage control voltage source inverter (VCVSI) as its power flow is controlled by the switching instant [9-11].

The main function of the CCVSI using RES for PCS is to improve harmonic distortions and power factor in the ac grid line, and achieve the energy saving used by the RES since extensive surveys quantify the problems associated with electric networks having non-linear loads. Hence, it is expected that the PCS will perform the following function.

1) Improved power quality: grid power conditioning including power quality control (PQC) such as maintaining power factor correction (>0.9) and harmonic mitigation (<5%) as per IEEE standard [12].
2) Active power support: load power conditioning includeing demand side management (DSM). In this function, the bi-directional CCVSI is responsible for controlling the active power between the AC grid and the DC bus including batteries, solar cells, fuel cells, etc.

Therefore, this paper deals with the grid-interactive CCVSI for PCS using the RES, which aims at the integration of the PQC and the DSM. The implementation system, which is operated by the polarized ramp time

† Corresponding Author: School of Electronic & Information Engineering, Kunsan National University, Kunsan, Korea. (merchin@kunsan.ac.kr)
* Research Lab., Hex-power System, Seoul, Korea.
** School of Electronic & Information Engineering, Kunsan National University, Kunsan, Korea. (srlee@kunsan.ac.kr)
Received August 12, 2005 ; Accepted October 11, 2005

(PRT) current control algorithm and the grid-interactive current control algorithm, is presented. 1KVA test model of the CCVSI has been built using IGBT controlled by a digital signal processor (DSP). To verify the proposed system, a comprehensive evaluation with theoretical analysis, simulation and experimental results is presented.

2. Grid-interactive current controlled voltage source inverter for power conditioning systems

The illustrated configuration of the parallel processing PCS using CCVSI is shown in Fig. 1.

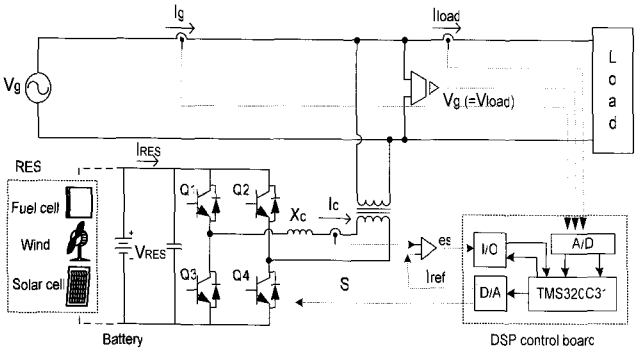

Fig. 1 Illustrated configuration of the proposed system

This system consists of a single-phase CCVSI, a DSP-based control module, an interfacing and sensing module, and an IGBT driver module. The CCVSI in the PCS generally connects to batteries and the RES such as solar cells, fuel cells, and so on. The output of the CCVSI is connected in parallel to a grid. The transformer will be utilized to boost the voltage based on the design requirement and transformer ratio to the target value. The transformer can be removed according to the DC input voltage. The main function of this system is to provide a unity power factor, lower THD and active power support. When a grid is available and is within the specified range of voltage and frequency, the grid will deliver the required active power to the load. The CCVSI will supply the required reactive power and active power from the RES within minimal power flow cycling through the battery.

2.1 Basic theory

The simplified equivalent schematic diagram can be presented as Fig. 2. As a CCVSI controls the current flow using the VSI switching instants, it is modeled as a current source. As the output voltage of the inverter is filtered, this current can be assumed to have only a fundamental frequency depending upon the grid (50 or 60 Hz). As the current generated from the CCVSI can be controlled independently from the voltage, the active and reactive power controls are decoupled. Hence, unity power factor operation for the entire range of the load is possible. This is one of the main advantages of CCVSI based PCS.

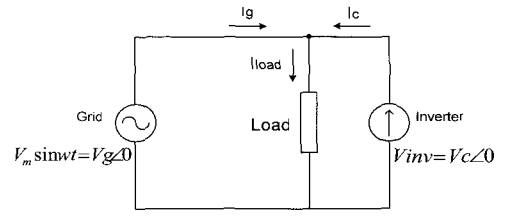

Fig. 2 The equivalent circuit of the proposed system

Fig. 3 shows the phasor diagram of a proposed system in the presence of the inductive load.

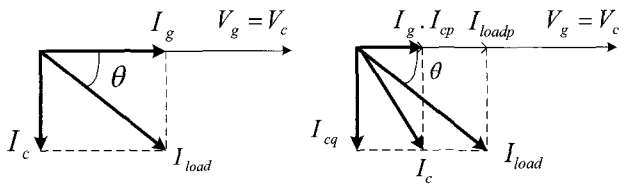

(a) PQC mode (b) DSM mode

Fig. 3 Phasor diagram of the proposed system at each operation mode at the inductive load

In Fig. 3 (a) is the phasor diagram of the PQC operation mode, and (b) is the phasor diagram of the DSM operation mode when the required active power of the load is supplied 50% each by the grid and the RES through the CCVSI. The CCVSI essentially becomes an AC current source, which controls the current magnitude and phase with respect to the grid voltage.

From Fig. 2, the load current (I_{load}) is continuously supplied by the current of the grid (I_g) and inverter (I_c), and it can be expressed as (1);

$$I_{load} = I_g + I_c \tag{1}$$

In the PQC, the active power of the load (P_{load}) demand should be equal to the grid power. Hence the required grid current can be rewritten as follows;

$$I_g^* = \mathrm{Re}[I_{load}] = \frac{\mathrm{Re}[P_{load}]}{V_g} \tag{2}$$

To manage the power flow of the entire system, the CCVSI current should be controlled to compensate the reactive current of the grid depending on the load condition Therefore, the CCVSI current must be controlled to meet the reactive current of the load demand as presented in (3);

$$I_c = I_{load} - I_g^* \tag{3}$$

In the DSM with RES, the required grid current in the DSM needs to be considered to include the RES output power (P_{RES}) in addition to the load power. As such, both the grid and the RES meet the load power. Equation (2) can be rewritten as follows;

$$I_g^* = \mathrm{Re}[I_{load}] - \mathrm{Re}[I_c] = \frac{(\mathrm{Re}[S_{load}] - P_{RES})}{V_g} \quad (4)$$

From equation (4), the CCVSI current should be controlled not only to compensate the reactive current of the grid depending on the load but also to reduce its active current corresponding to the RES condition for the DSM. Thus the CCVSI current can be determined by Equations (3) and (4).

2.2 System description and control strategy

From Fig. 1, the main elements are the full-bridge type VSI, a battery bank, an interfacing and sensor module, an IGBT driver and protection circuit, and a DSP controller. A summary of the system components is given in Table 1.

Table 1 Components of the system

Component	Part Number	Manufacturer
IGBT	2MB50L060	Fuji
Battery	ITX40	ATLASBS
DSP	TMS302C31	TI
Voltage sensor	LV25P	LEM
Current sensor	LA25P	LEM
Protection and dead time circuit	XC9536XL	Xillings
Gate driver	EXB841	Fuji

IGBT modules are selected as the power switch due to their high switching frequency, low loss, and minimal gate drive requirements. The increasing power rating of the IGBT allows for application of the system up to thousands of KVA. A DC voltage source is realized with the battery by using the RES, which is optional, as indicated in Fig. 1. A Texas Instruments DSP, the TMS302C31, acts as the system controller. The DSP receives digital input data from the MAX122 analog-to-digital (A/D) converter. The DSP sends analog output data from the AD664 digital-to-analog (D/A) converter. The control block diagram of the proposed system using Equations (3) and (4) is presented in Fig. 4. The control algorithm of the system consists of two current control algorithms, the grid-interactive control algorithm and the PRT current control algorithm. The grid-interactive control sequence is used to sense the voltage (V_{load}) and current (I_{load}) of the load and voltage (V_{RES}) and current (I_{RES}) of the RES. The PRT current control sequence is used to sense and feedback the CCVSI current (I_c) and the PWM switching sequence.

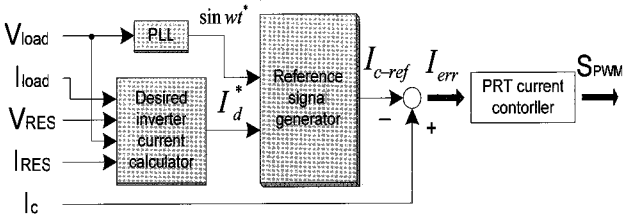

Fig. 4 Control block diagram of the proposed system

The grid-interactive current control scheme samples the load voltage for synchronization using a PLL. The samples of load current, RES current (I_{RES}) and voltage (V_{RES}) are utilized to generate the desired CCVSI current amplitude (I^*_d) using Equations (3) and (4). After generating the reference current signal ($I_{c\text{-}ref}$), the reference current is compared to the instantaneous CCVSI current, in order to generate the error current (I_{err}). The error current is then given to the PRT current controller to generate the desired instantaneous switching PWM (S_{PWM}).

2.2.1 PRT current control algorithm

PRT current control was developed in an effort to find a zero average current error (ZACE) method with a fixed switching frequency. This method uses only the current error signal to determine switching instants, and aims to maintain a narrow switching frequency band [10-11]. In the PRT current control loop, the actual CCVSI current is forced to follow the reference current. The actual CCVSI current is measured with an instantaneous measurement, and is subtracted from the reference current to an error signal. Fig. 5 indicates the current error signal at each time period.

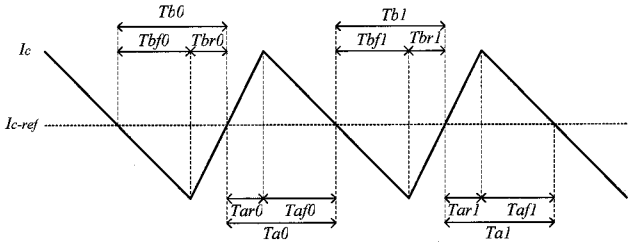

Fig. 5 Current error signal at each period

The PRT current control scheme is explained by reference to the current error signal in Fig. 5. Assuming a fixed inductance, and negligible variance in the current reference within the switching period, the constant slopes over that switching period. Ta is the period of time when Ierr is above zero and Tb is the period of time when Ierr is below zero. If Ta can be made equal to Tb, then the area of the current error signal above zero will equal the area of the current error signal below zero, and the average value

of the current error signal over that switching period will be zero. The PRT current control scheme assumes that the error current is made up of linear segments and calculates the next switching instant using duty cycles and time information.

To determine T^{*}_{ar1}, the immediately previous $T^{\wedge}_{ar0}$ and $T^{\wedge}_{a0}$ are used. Similarly, to determine T^{*}_{bf1}, the immediately previous $T^{\wedge}_{bf0}$ and $T^{\wedge}_{b0}$ are used as follows;

$$T^{\#}_{ar1} = (\frac{T^{\wedge}_{ar0}}{T^{\wedge}_{a0}})(\frac{T_{sw}}{2}) \quad (5)$$

$$T^{\#}_{bf1} = (\frac{T^{\wedge}_{bf0}}{T^{\wedge}_{b0}})(\frac{T_{sw}}{2}) \quad (6)$$

where, ^ indicates a measured value
# indicates a calculated (or desired) value

Fig. 6 shows the PRT current control illustrated in the functional block diagram. Es is a binary signal indicating the polarity of current error signal Ierr. Es is high when I_{err} is positive and low when I_{err} is negative. PWM switching signal S is a binary signal used as a command for the inverter main switches. Fig. 7 depicts the operation waveforms of the PRT current control at each time period.

Ta : an integrator (or counter) to measure Ta
Tar : an integrator (or counter) to measure Tar
Ta Ramp : an integrator (or counter) for creating a ramp with a slope proportional to Ta
Tb : an integrator (or counter) to measure Tb
Tbf : an integrator (or counter) to measure Tbf
Tb Ramp : an integrator (or counter) for creating a ramp with a slope proportional to Tb

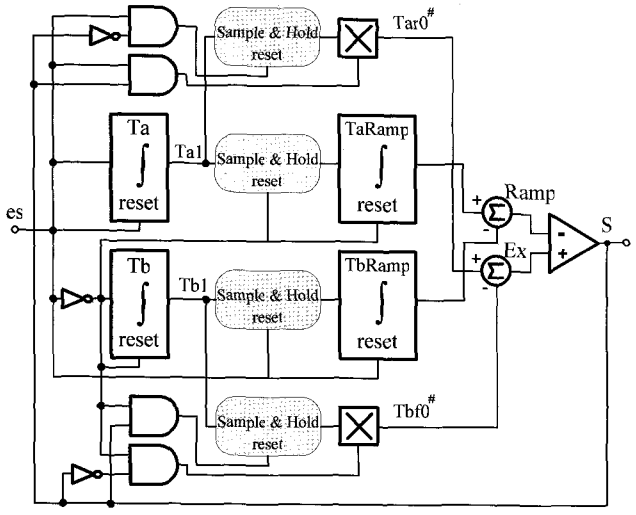

Fig. 6 Functional diagram of the PRT current control

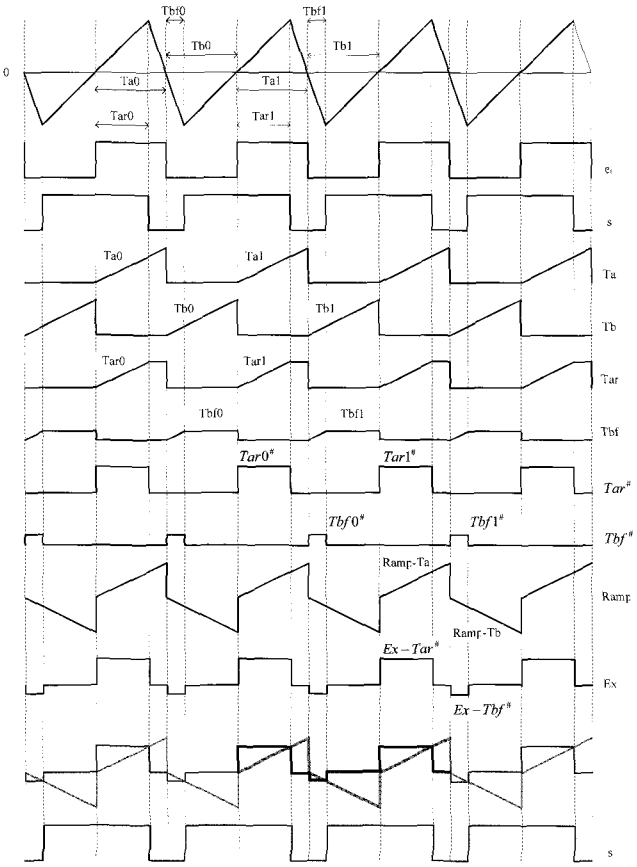

Fig. 7 Operation waveforms of the PRT current control

2.2.2 Grid-interactive current control algorithm

In this paper, a digital system based on the TMS320C31 DSP board has been used to implement the grid-interactive current control algorithm. From the control block diagram (Fig. 4), the flow chart of the grid-interactive current control algorithm can be shown as in Fig. 8. It is indicated that the main software is cycles after the system has initialized and waiting for interruption. The DSP320C31 provides an internal timer interruption service routine (TISR), which is caused by the TSTAT bit of the timer control register. The frequency of TISR depends on whether the timer is set up. The input data can be updated at every period of TISR, instantaneously. In this paper, the one-period of TISR is decided at 92.6[us] and it is performed at the iteration of 180 during one period for the grid voltage (frequency 60[Hz]). This consists of three primary parts in the TISR for the DSP to achieve the grid-interactive current control strategy. First, all operations require scaling the value from the A/D converter and addressing the memory in a DSP control board. In this paper, the sampling frequency is 10.8[KHz] to perform the sample points of 180 for one period of the grid. Second, following zero crossing detection (ZCD), required data are calculated, such as P_{load}, P_{RES}, V_{rms} and the synchronization period (sinwt*) associated with the grid. If ZCD is 0, it is

written to register what input data is integrated, and the number of TISR is counted. IF ZCD is 1, the P_{load}, P_{RES}, V_{rms} and sinwt* are calculated by using the stored data during one period of the grid, and then the register of data and counter is reset. Third, depending on the power of the RES, the operation mode is selected. And then the desired grid current and reference inverter current are calculated. Finally, this reference signal($I_{c\text{-}ref}$) is sent to the PRT controller of the inverter by using the D/A converter.

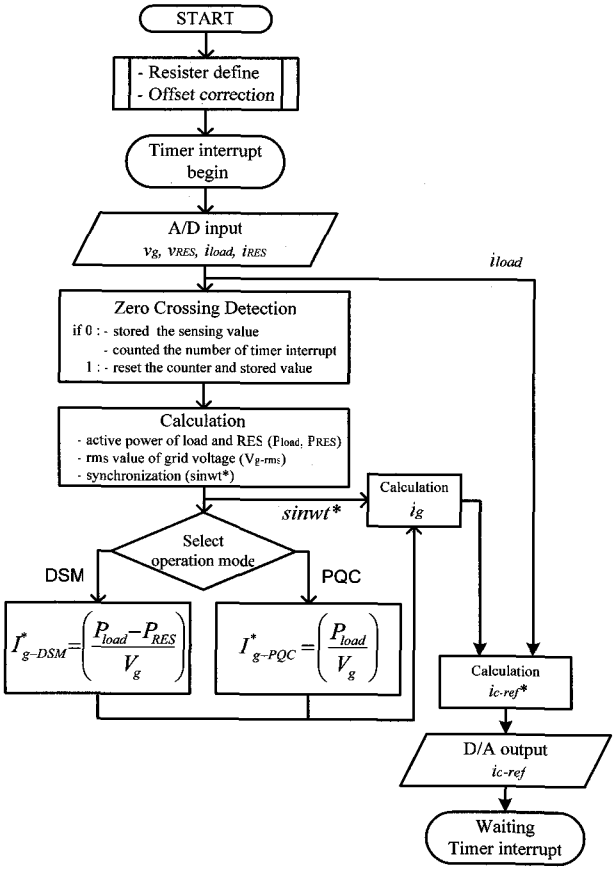

Fig. 8 Flowchart for grid-interactive control algorithm

3. Simulation results

A PSim simulator was used for simulation in order to verify the proposed system. Linear and non-linear load conditions for the simulation were determined to be the 1KVA load capacity. Table 2 presents the simulation condition and parameter values identical with the experimental hardware in order to compare the results.

Table 2 Simulation condition and parameters

Parameter	Value	Parameter	Value
Vac	200Vrms	Vdc	180V
fs	60Hz	Fsw	5kHz
Lc	6mH	Transformer	1:2

Where, fs is the fundamental frequency, fsw is the switching frequency, Lc is the coupled inductor.

The waveform of the PQC operation mode at resistive, inductive and non-linear load conditions is shown in Fig. 9 (a), (b), (c) and (d), respectively.

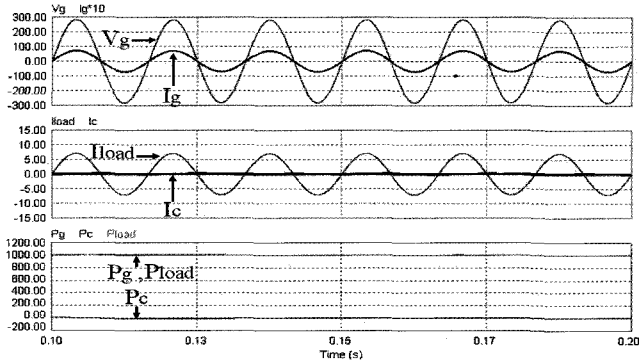

(a) When the pure resistive load is adopted as R= 40[Ω]

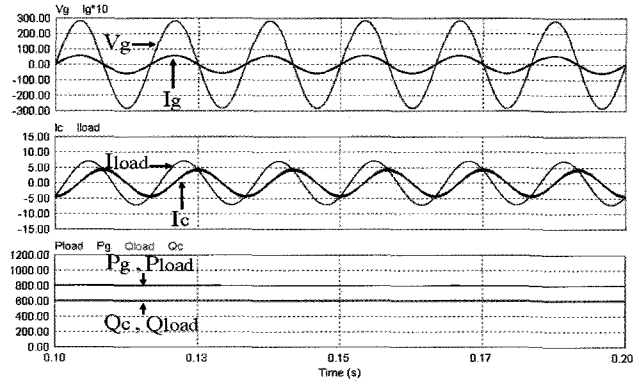

(b) When the inductive load is adopted as Z= 40∠36.7°[Ω]

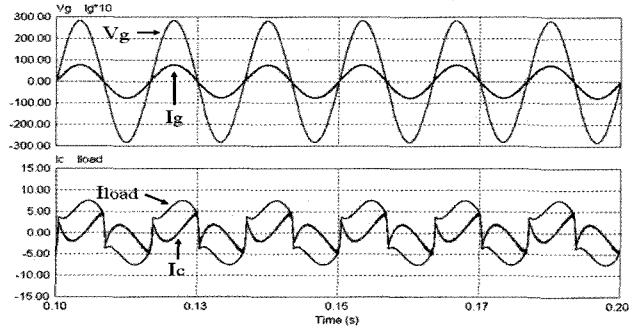

(c) When the non-linear load is adopted as the diode bridge rectifier with RL

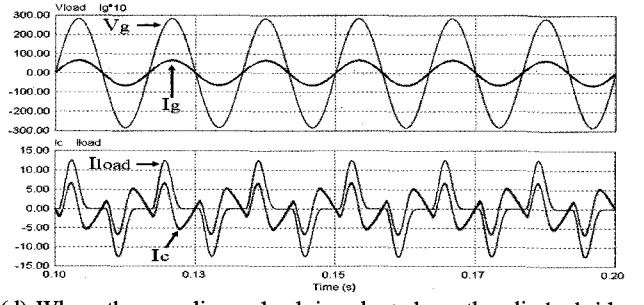

(d) When the non-linear load is adopted as the diode bridge rectifier with RLC

Fig. 9 Waveforms of PQC operation mode

Where V_g is the voltage waveforms of the grid, and I_g, I_c and I_{load} are current waveforms of the grid, CCVSI and load respectively.

As in Fig. 9 (a), the active power flows into the load from the grid. And, the CCVSI has no need to control the reactive power since the load is pure resistive. Fig. 9 (b) shows the PQC operation of the system in the presence of an inductive load (Z= 48∠36.7°[Ω]). The active power is also supplied from the grid to the load. In this case, the required reactive power (600Var) can be supplied by the CCVSI. Fig. 9 (c) and (d) indicates that the CCVSI can provide all the reactive power and harmonic current of a load demanded by the non-linear load and hence the grid supplies only the remaining active power. In this case, the CCVSI prevents any low order harmonics from being injected into the grid. The harmonic spectrum of the grid current with the non-linear load in Fig. 9 (c) and (d) are presented in Fig. 10.

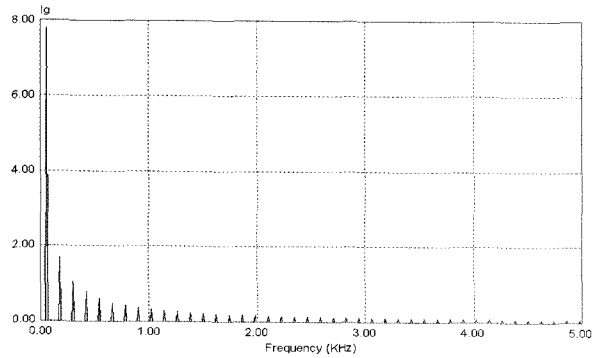

(a) Without PQC

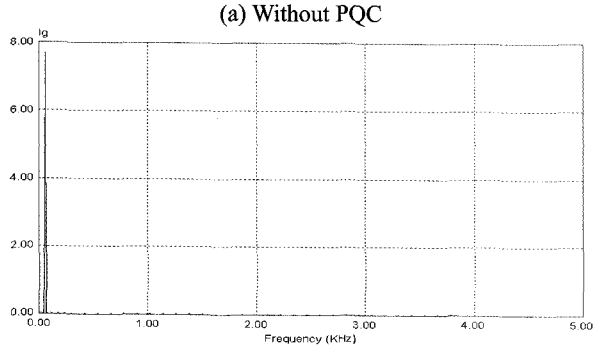

(b) With PQC

(i) When the non-linear load is as the diode bridge rectifier with RL

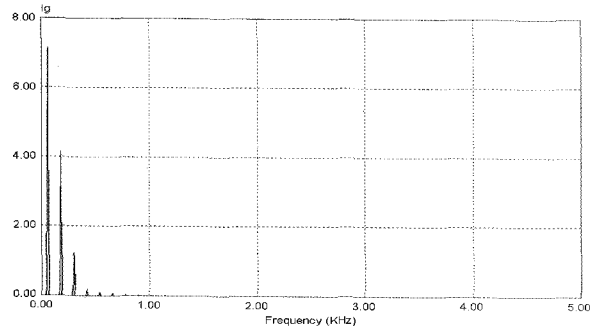

(c) Without PQC

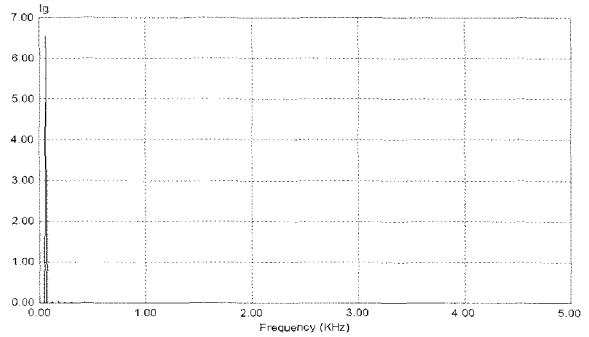

(d) With PQC

(ii) When the non-linear load is as the diode bridge rectifier with RLC

Fig. 10 The harmonic spectrum of the grid current

Fig. 10 (a) and (c) shows the harmonic spectrum of the grid current in the system without PQC. In this case, all the reactive power associated with low order harmonics must be supplied by the grid (Fig. 10 (a) and (c), THD=32.2% and 60.8%). But it can be remarkably compensated as THD =3.2% and 1.1% with PQC by using the CCVSI as shown in Fig. 10 (b) and (d). The above signifies that the CCVSI can achieve unity PF and the satisfied THD of voltage and current in the entire load condition. This means the proposed system can meet the IEEE standard (less than 5% of THD and bigger than 0.9 of power factor).

The waveform of the DSM operation at linear and non-linear load conditions is shown in Fig. 11 (a), (b) and (c), respectively. Where P_g, P_c and P_{load} are the active power waveforms of the grid, CCVSI and load, and Q_c and Q_{load} are the reactive power waveforms of CCVSI and load, respectively.

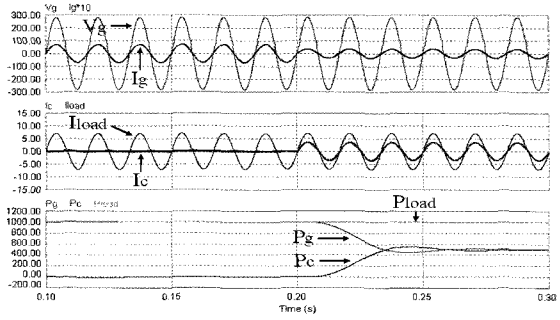

(a) When the pure resistive load is adopted as R= 40[Ω]

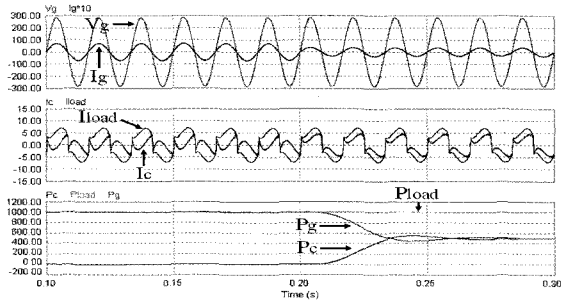

(b) When the non-linear load is adopted as the diode bridge rectifier with RL

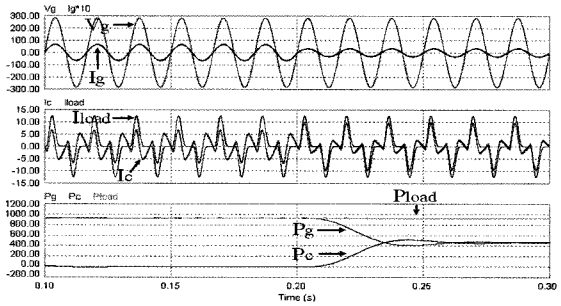

(c) When the non-linear load is adopted as the diode bridge rectifier with RLC

Fig. 11 Waveforms of DSM operation mode

As indicated in Fig. 11 (a), the grid should supply all the active power (1kw) required from the load when in normal state. If the RES is available, the proposed system can be controlled to DSM operation mode, which supplies a certain part of the required load power by the CCVSI, which is connected in the DC bus and the battery bank. In this paper, for example, the grid supplied 50% of the required active power while the CCVSI handled the balance of the required load power. Fig. 11 (b) and (c) indicates that the grid supplies almost the entire active power demanded. And the CCVSI supplies the active and reactive power required by the load. This indicates that the proposed system can achieve the DSM operation and compensate the current harmonics and reactive power at the same time.

4. Experimental results

In order to confirm the above mentioned simulation results pertaining to system performance, the prototype PCS (1 KVA) for the experiment was constructed to be identical to the simulation parameters and the operating condition with the simulation. Fig. 12 shows a schematic diagram of the experimental setup used to test the performance of the power electronic interface.

Fig. 13 shows a PCS that was prototyped to examine the above analytical and simulation analysis. The system specifications are given in Table 1.

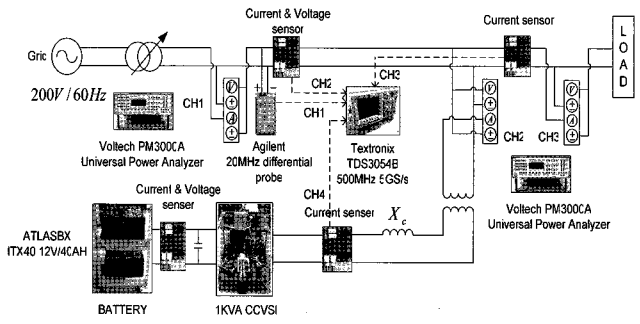

Fig. 12 Schematic diagram of the experimental setup

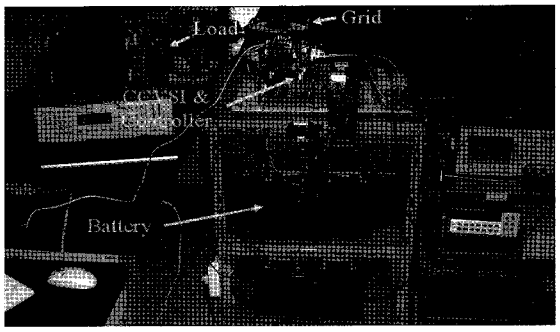

Fig. 13 Photograph of the experimental setup

The experimental waveform of the PQC operation mode at resistive, diode bridge rectifier with RL and diode bridge rectifier with RLC load condition is indicated in Fig. 14 (a) (b), and (c) respectively.

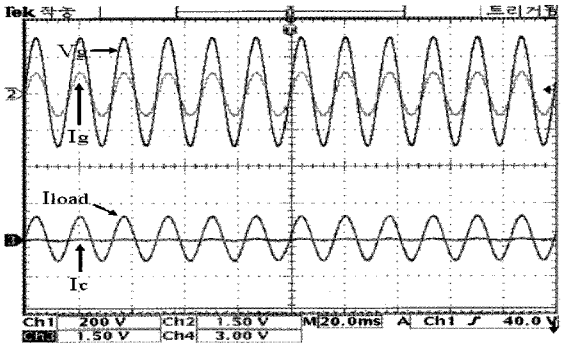

(a) When the pure resistive load is adopted as R= 40[Ω]

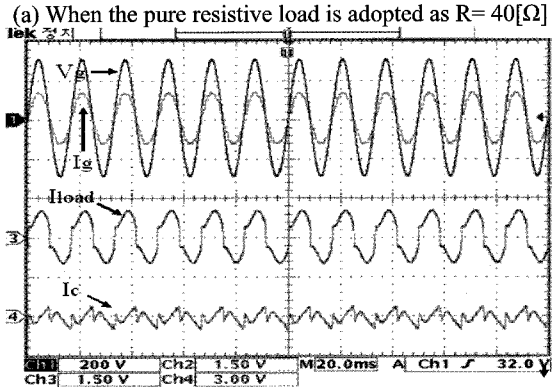

(b) When the non-linear load is adopted as the diode bridge rectifier with RL

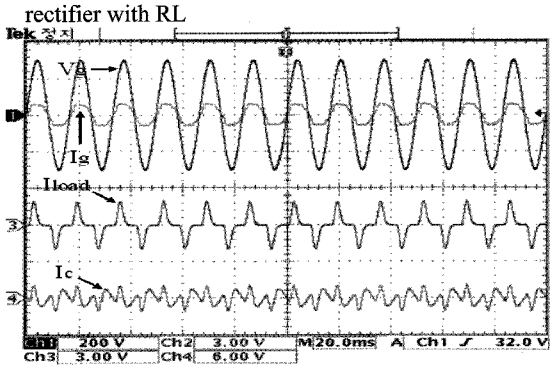

(c) When the non-linear load is adopted as the diode bridge rectifier with RLC

Fig. 14 Experimental waveform results of PQC operation mode

Fig. 14 illustrates that the CCVSI supplies the reactive power and harmonic current demanded by the load and the grid supplies the load active power. These results comply with the simulation results (Fig. 9). Using the Voltech (PM3000 A) it measures a power factor of over 0.98 for a proposed system at the whole load condition. The Tektronix (TDS305 4B) digital oscilloscope has been used to capture the following results. The current value is volt (V) because LEM (LA25P) current sensor output converted current to voltage. The current division ratio is 1(scope value): 5(real value). And, the CCVSI current I_c is the primary current of the transformer. Fig. 15 presents the current harmonic spectrum of the grid current from zero to 5 [kHz] when the non-linear load is identical to the simulation condition in Fig. 10.

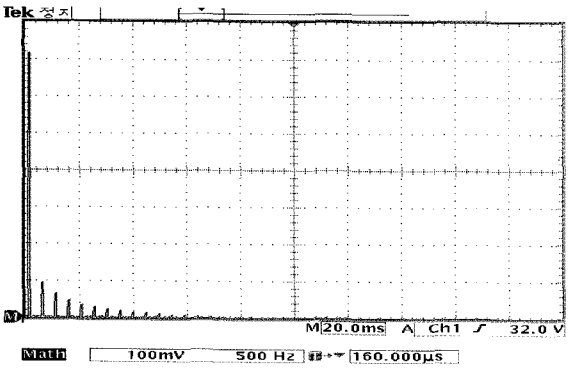

(a) Without PQC

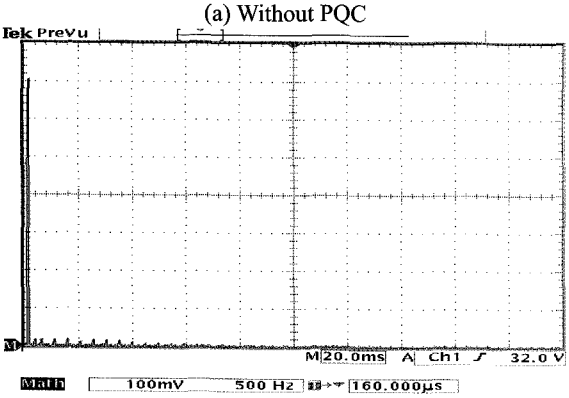

(b) With PQC

(i) When the non-linear load as the diode bridge rectifier with RL

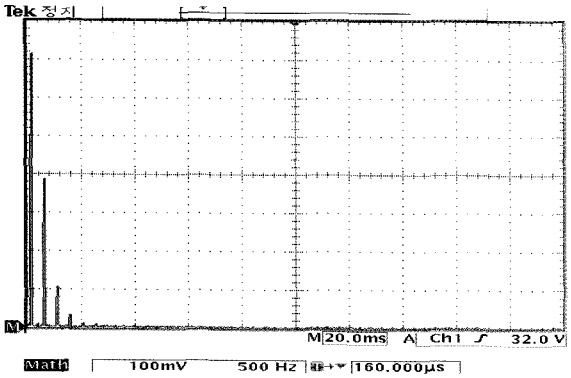

(c) Without PQC

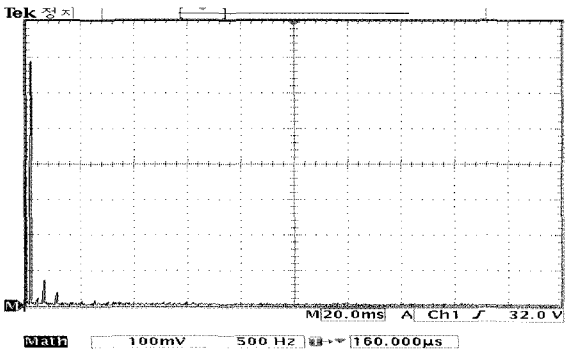

(d) With PQC

(ii) When the non-linear load as the diode bridge rectifier with RLC

Fig. 13 Experimental FFT results of the grid current

The Tektronix (TDS3054B) digital scope already has a FFT module. Compared with the current harmonic without PQC (THD=33.5% and 62.1%), it measured as THD=4.2% and 4.8% with PQC by using the CCVSI as shown in Fig. 15 (b) and (d), respectively. It indicates that the CCVSI offers the best performance in reducing the grid current harmonic distortion. These results also confirm the validity of the simulation (Fig. 10).

The experimental waveform of the DSM operation at linear and non-linear load condition is presented in Fig. 16 (a), (b) and (c), respectively. This suggests that the grid supplies almost the entire active power demanded. And also, the CCVSI supplies the active and reactive power required by the load. These results comply with the simulation results in Fig. 11.

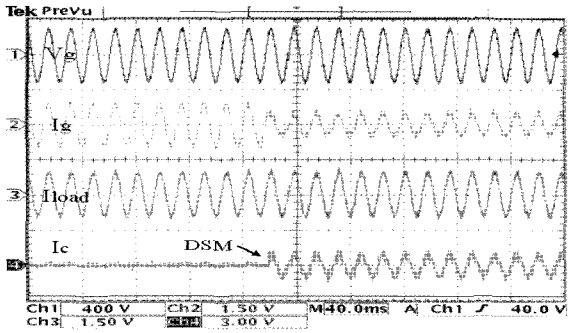

(a) When the pure resistive load is adopted as R= 40[Ω]

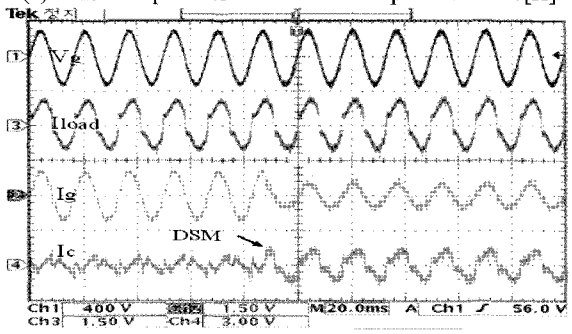

(b) When the non-linear load is adopted as the diode bridge rectifier with RL

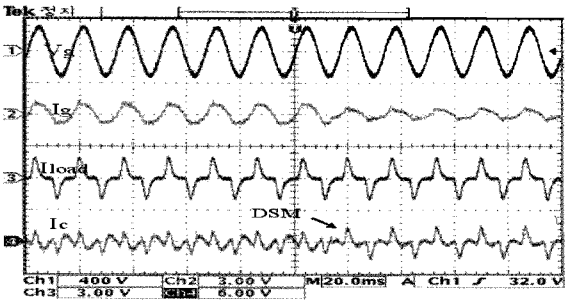

(c) When the non-linear load is adopted as the diode bridge rectifier with RLC

Fig. 16 Experimental waveform results of DSM operation mode

The above signifies simulation and experimental results of the proposed system and can be summarized as follows:

- Power quality improvement (PQC operation): The proposed system can provide good reactive power support and decouple from the active power. Hence, unity power factor and low order harmonic mitigation is possible.
- Active power Support (DSM operation): The proposed system can offer bi-directional power flow between the DC and AC bus without deteriorating the system performance. And, the proposed system can achieve the DSM operation and compensate the current harmonics and reactive power simultaneously.

5. Conclusion

The parallel processing PCS by using the CCVSI has become very popular. As it is inherently efficient, compact and economical, it offers numerous functions requiring a minimum number of power conversions. Therefore, in this paper, the grid-interactive CCVSI for parallel processing PCS with RES, which is operated by grid-interactive and PRT current control algorithm, was presented. And to verify the design consideration, theoretical analysis and computer simulations, 1KVA test model of the CCVSI has been implemented using IGBT controlled by DSP (TMS302C31). The detailed experimental results not only verify system theory and simulation but also satisfy the IEEE recommended requirement for electric power quality. Therefore, the parallel processing PCS by using the CCVSI can be applicable to a power quality control to reduce harmonic current and improve power factor, and a demand side management to supply active power simultaneously.

Acknowledgements

This work was partially supported by the Brain Korea 21 Project of Kunsan National University.

References

[1] M. Prodanovi and T.C. Green, "Control and filter design of three-phase inverters for high power quality grid connection," *IEEE Trans. Power Electronics*, vol. 18, no. 1, pp. 373-380, Jan., 2003.

[2] A. Baronian and S. Dewan, "An adaptive digital control of current source inverter suitable for parallel processing inverter systems," *Conf. Rec. of IEEE IAS 1995-Annual Meeting,* vol. 3, pp. 2670-2671, Oct., 1995.

[3] H. Dehbonei, "Power conditioning for distributed renewable energy generation," Ph.D thesis in School of Electrical and Computer Eng., Curtin University of Technology, June, 2003.

[4] M. Dai, M.N. Marwail, J.W. Jung and A. Keyhani, "Power flow control of a single distributed generation unit with nonlinear local load," *Conf. Rec. of IEEE PES 2004,* vol. 1, pp. 398-403, Oct., 2004.

[5] T. Kawabata, N. Sashida, Y. Yamamoto, K. Ogasawara and Y. Yamasaki, "Parallel Processing Inverter System," *IEEE Trans. power Electronics*, vol 6, no. 3, pp. 442-450, July, 1991.

[6] M. N. Marwali and A. Keyhani, "Control of distributed generation systems-Part I: Voltages and Currents control," *IEEE Trans. Power Electronics*, vol. 19, no. 6, pp. 1541-1550, Nov., 2004.

[7] G. Ledwich and A.Ghosh, "A flexible DSTATCOM operating in voltage or current control mode," *IEE proceedings Generation, Transmission and Distribution*, vol. 149, no. 2, pp. 215-224, March, 2002.

[8] Z.Chen and E.Spooner, "Voltage source inverters for high -power, variable-voltage DC power sources," *IEE Proceedings on Generation, Transmission and Distribution*,vol. 148, no. 5, pp. 439-447, Sept., 2002.

[9] L.J. Borle, M.S. Michael and C. V. Nayar, "Development and testing of a 20-kW grid interactive photovoltaic power conditioning system in western Australia," *IEEE Trans, Industry Applications*, vol. 33, no. 2, pp. 502-508, March, 1997.

[10] L. J. Borle and C. V. Nayar, "Ramptime current control," *Conf. Rec. of APEC 1996,* vol. 2, pp. 828-834, March, 1996.

[11] S. R. Lee, C. H. Jeon and S. H. Ko, "A new current controlled Inverter with ZVT switching," *Conf. Rec. of ICPE 2001*, vol. 1, pp. 309-313, Oct., 2001.

[12] IEEE Standard 1159, "Monitoring Electric Power Quality," *IEEE Standards Board*, June, 1995.

Sung-Hun Ko

He received his B.Sc. and M.Sc. degrees from the Department of Control and Instrumentation Engineering, Kunsan National University, Korea in 1998 and 2000, respectively, and is currently a Ph.D degree candidate in the School of Electronics and Information Engineering at the same institution. He is also currently working as a Visiting Research Fellow with the Department of Electrical and Computer Engineering at the Curtin University of Technology, Australia. From 2000 to 2001, he was with the Research Laboratory of Seo-Young Electronics, Inc., Korea. His research interests include renewable energy based distributed generation systems, power factor correction, inverter control and neural networks.

Young-Chan Shin

He received his B.Sc. and M.Sc. degrees from the School of Electronics and Information Engineering, Kunsan Nation-al University, Korea in 2003 and 2005, respectively. He is currently working in the Research Laboratory of Hex-power System, Inc., Korea. His research interests include renewable energy based distributed generation systems and inverter control.

Seong-Ryong Lee

He received his B.Sc. and M.Sc. degrees in Electrical Engineering from Myong-Ji University, Korea in 1980 and 1982, respectively and his Ph.D degree from Chonbuk National University, Korea, in 1988. Since 1990, he has been a Professor with the School of Electronics and Information Engineering at Kunsan National University, Korea. He was a Visiting Professor with the Department of Electrical and Computer Engineering at Virginia Tech., USA from 1997 to 1998. Currently he is working as a Visiting Professor with the Department of Electrical and Computer Engineering at the Curtin University of Technology, Australia until 2005. His research interests include soft-switching inverters, power factor correction, switch mode power supply and renewable energy based distributed generation systems.